

Cite this: *Analyst*, 2012, **137**, 3126

www.rsc.org/analyst

PAPER

Amperometric detection of hypoxanthine and xanthine by enzymatic amplification using a gold nanoparticles–carbon nanohorn hybrid as the carrier

Lei Zhang, Jianping Lei,* Jing Zhang, Lin Ding and Huangxian Ju

Received 29th February 2012, Accepted 19th April 2012

DOI: 10.1039/c2an35284b

A novel gold nanoparticles–single-walled carbon nanohorn (GNPs–SWCNH) hybrid was synthesized for the construction of an amperometric biosensing platform. The GNPs–SWCNH hybrid was stable in aqueous solution for at least two weeks, and was characterized with scanning electron microscopy, transmission electron microscopy, and electrochemical impedance spectroscopy. The average diameter of GNPs *in situ* synthesized on the SWCNH was 5–8 nm, and the good interaction between GNPs and SWCNH was confirmed by ultraviolet-visible absorption spectroscopy. The GNPs–SWCNH immobilized on a platinum electrode showed high electrochemical activity toward the oxidation of hydrogen peroxide and uric acid with low applied potentials. Combining with the enzymatic reaction of xanthine oxidase (XOx), a biosensor for hypoxanthine and xanthine was constructed. The XOx–GNPs–SWCNH-based biosensor exhibited good responses to hypoxanthine and xanthine with the linear ranges of 1.5 to 35.4 and 2.0 to 37.3 μM , and the detection limits of 0.61 and 0.72 μM , respectively. The recovery test showed acceptable results. The gold nanoparticles functionalized carbon nanohorns provided a promising way to construct an electrochemical platform for sensitive biosensing.

Introduction

Single-walled carbon nanohorns (SWCNHs), as a relatively new kind of carbon materials, have a large number of individual tubules to form spherical bundles with an average size range of 50–100 nm. The SWCNHs with high purity can be prepared in the absence of metallic catalysts. This material has aroused considerable attention in a variety of research areas, due to its excellent conductivity and biocompatibility and special structural characters compared to carbon nanotubes,¹ carbon nanosheets,² and graphene.³ For example, SWCNHs have been operated as a new solid phase extraction adsorbent,⁴ pseudostationary and stationary phases in capillary electrophoresis,⁵ architectures of supercapacitors,⁶ and applied in mini-biofuel cells.⁷ The SWCNH modified electrodes display excellent electrocatalytic activity for simultaneous determination of uric acid, dopamine, and ascorbic acid.⁸ More interestingly, the cone-shaped tips of SWCNHs can provide plentiful sites for immobilization of biomacromolecules, and the three-dimensional recognition for biosensing.

Recently, great efforts have been devoted to the functionalization of SWCNHs for specific recognition of biomolecules. The main functionalization approaches include three aspects: (1)

noncovalent assembly of biomolecules *via* hydrophobic interaction and π – π stacking, which can avoid destruction of the conjugated skeleton and loss of electronic properties of the SWCNHs;⁹ (2) covalent binding of biomolecules through amide bonds after SWCNHs were treated with an acid;¹⁰ (3) hybridization of SWCNHs with metal nanoparticles such as platinum or palladium nanoparticles by an arc discharge process.^{11,12} In this work, a facile method was developed for the functionalization of SWCNHs by *in situ* deposition of gold nanoparticles (GNPs) on pristine SWCNHs. The formed GNPs–SWCNH hybrid was further used for immobilization of xanthine oxidase (XOx), leading to a biosensor for the detection of hypoxanthine and xanthine.

Hypoxanthine, a natural purine derivative, is found as a potential marker widely present in plants and animals, while xanthine is a metabolic intermediate of nucleotides, which can be generated from hypoxanthine by XOx. The determination of hypoxanthine and xanthine is of great importance in food chemical industries,¹³ medical and biological aspects. Although methods such as high performance liquid chromatography,¹⁴ liquid chromatography-mass spectrometry¹⁵ and electrochemiluminescence¹⁶ have been used for the detection of hypoxanthine, alternative protocols with high sensitivity, simplicity and ease of miniaturization, like electrochemical biosensors, are in urgent need.

Based on the good biocompatibility, high surface-to-volume ratio, and excellent conductivity of GNPs–SWCNH, the hybrid

State Key Laboratory of Analytical Chemistry for Life Science, Department of Chemistry, Nanjing University, Nanjing 210093, P.R. China. E-mail: jpl@nju.edu.cn; Fax: +86 25 83593593; Tel: +86 25 83593593

could be conveniently immobilized on a platinum electrode for assembly of enzyme molecules. This hybrid modified electrode exhibited good electrocatalytic activity toward oxidation of both H_2O_2 and uric acid (UA), the enzymatic products from the oxidation reaction of hypoxanthine or xanthine by dissolved oxygen. Thus a sensitive biosensor was prepared by further assembling XOx on the hybrid modified electrode surface. This biosensor could be applied in the analysis of real samples with good recoveries. The GNPs–SWCNH hybrid provided a promising platform for detection of trace amounts of a wide variety of analytes in bioanalysis and biosensing.

Experimental

Materials and reagents

SWCNHs were kindly provided by Professor Sumio Iijima in Japan. Poly(diallyldimethylammonium chloride) (PDAA, 20%, w/w in water, M_w : 200 000–350 000), xanthine oxidase (EC 1.1.3.22, from a microbial source, 8.1 U mg^{-1}), hypoxanthine ($\geq 99\%$) and xanthine ($\geq 99\%$) were purchased from Sigma Chemical Co. (MO, USA).

The solution of diluted H_2O_2 was daily prepared prior to detection. All other reagents were of analytical grade. All aqueous solutions were prepared using ultra-pure water (≥ 18 M Ω , Milli-Q, Millipore). The buffer for the assay was 50 mM phosphate buffer saline (PBS) prepared by mixing stock-standard solutions of Na_2HPO_4 and NaH_2PO_4 .

Instrumentation

The scanning electron microscopic (SEM) image was obtained using a Hitachi S-4800 scanning electron microscope (Japan). The transmission electron microscopic (TEM) images were gained on a JEM-2100 TEM (JEOL, Japan). Electrochemical impedance spectroscopy (EIS) was carried out on a PGSTAT30/FRA2 system (Autolab, Netherlands) using the three-electrode setup in 0.1 M KNO_3 containing 5 mM $\text{Fe}(\text{CN})_6^{3-/4-}$ (1 : 1). The impedance spectra were recorded within the frequency range of 10^{-2} to 10^5 Hz. Ultraviolet-visible (UV-vis) absorption spectra were recorded on a UV-3600 type UV-vis-NIR spectrophotometer (Shimadzu instruments, Japan). X-ray photoelectron spectra (XPS) were obtained using an ESCALAB 250 spectrometer (Thermo-VG Scientific, USA) with an ultra-high vacuum generator. Cyclic voltammetric and amperometric experiments were performed on a CHI 650D electrochemical analyzer (Co. CHI, USA) with a modified platinum working electrode, a platinum auxiliary electrode and a saturated calomel reference electrode. All measurements were carried out at room temperature.

Preparation of GNPs–SWCNH hybrid

4 mg SWCNHs were dispersed in a 40 mL aqueous solution containing 2.5×10^{-4} M trisodium citrate by sonication for 60 min. 0.4 mL 1% $\text{HAuCl}_4 \cdot 3\text{H}_2\text{O}$ was added to the solution with gentle stirring for 10 min. Then 1.2 mL of 0.1 M ice-cold NaBH_4 solution was added to the mixture solution under stirring at 0°C . After stirring for an additional 2 h, the black solid was separated by centrifuging at 12 000 rpm, washed with water for several cycles, and then dried overnight at 80°C .

Preparation of the biosensor

The platinum electrode (1 mm radius, CH Instrument, USA) was consecutively polished to a mirror finish using 0.3 and 0.05 μm alumina slurry, followed by thorough washing with ultrapure water. After successive sonication in ethanol and ultrapure water, the electrode was washed with ultrapure water and blown to dryness using N_2 stream.

1 mg GNPs–SWCNH was dispersed in 1 mL water and sonicated for 5 min to acquire a well-dispersed suspension. 3 μL of the suspension was dropped on the pretreated platinum electrode surface and dried in air, then 3 μL of 4 mg mL^{-1} XOx solution and 3 μL of 0.5% PDAA were in turn cast on the GNPs–SWCNH modified electrode to obtain the enzyme immobilized biosensor. The formed PDAA layer was utilized to maintain the stability of the modified electrode. The prepared biosensor was stored in 50 mM PBS at 4°C in a refrigerator when not in use.

Sample preparation

The locally purchased fish sample was treated as in our previous report.¹⁶ Briefly, a piece of fish meat (4–5 g) was ground and homogenized in 15 mL of ultrapure water for 30 min. The solution was then filtered through a filter membrane (0.22 μm pore size). Ultrapure water was then added into the filtrate to produce a total volume of 50 mL homogenized sample solution. A mixture containing equal volumes of the fish extract and 0.1 M PBS was used for further analysis. The sample solutions were prepared prior to the experiment.

Results and discussion

Characterization of GNPs–SWCNH hybrid

SWCNHs have a dahlia-like nanostructure with the diameter of about 80–100 nm. The formed GNPs–SWCNH clearly displayed the nanoparticles homogeneously deposited on the surface of pristine SWCNHs, which increased the surface area and produced a nanoporous structure (Fig. 1A and B). The average size of the GNPs was 5–8 nm (Fig. 1B). Compared with pure SWCNHs (Fig. 1C), the structure of SWCNHs was not destructed after depositing GNPs, which afforded an excellent conductivity for the preparation of electrochemical biosensors.

The UV-vis spectra of both GNPs–SWCNH and SWCNHs showed an absorption peak at 262 nm (Fig. 2), which came from the absorption of SWCNHs. The GNPs–SWCNH showed another slight absorption peak at around 540 nm (Fig. 2, curve a), indicating that GNPs were immobilized on SWCNHs. In comparison with the peak at 512 nm of free GNPs,¹⁷ this peak

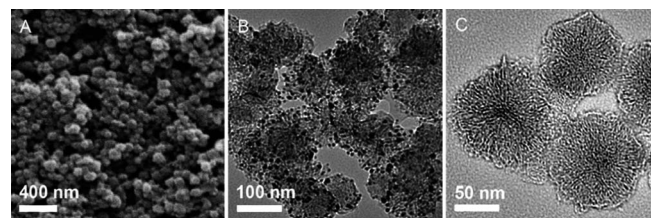


Fig. 1 (A) SEM and (B) TEM images of GNPs–SWCNH, (C) TEM image of SWCNHs.

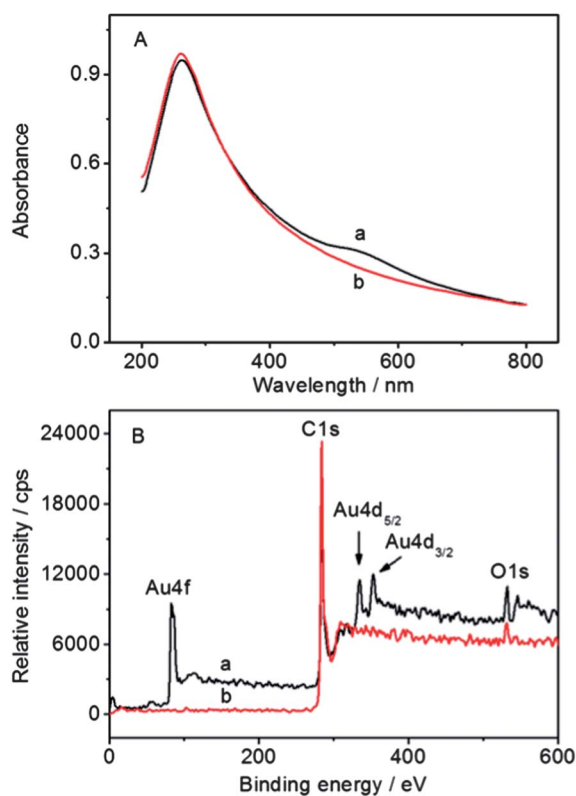


Fig. 2 (A) UV-vis absorption spectra and (B) XPS spectra of GNP-SWCNH (a) and SWCNHs (b).

was red-shifted, which indicated a strong interaction *via* π - π^* transitions between the GNPs and SWCNHs.^{9a} This result was consistent with the cases of GNPs-carbon nanomaterials.¹⁸

As shown in Fig. 2B, the survey XPS spectrum of SWCNHs exhibited the C1s and O1s peaks at the binding energies of 284 and 531 eV, respectively, and the atomic percentage of C1s and O1s are 98.05% and 1.95%. The small amount of O should come from the impurity during the preparation. After GNPs *in situ* synthesized on the surface of SWCNHs, the survey XPS spectrum of GNP-SWCNHs (Fig. 2B, curve a) displayed three new peaks of Au 4f, 4d_{5/2} and 4d_{3/2} at the binding energies of 83, 334 and 353 eV, respectively. This result further confirmed the formation of metallic Au on the SWCNH surface, which could enhance the conductivity and surface area for the preparation of the biosensor.

The contact angle measurement could represent the biocompatibility of the substrate. As shown in Fig. 3A, the contact angles of bare (Fig. 3A, photo a) and SWCNH modified (Fig. 3A, photo b) substrates were measured to be 60.7° and 49.5°, respectively. The GNP-SWCNH hybrid (Fig. 3A, photo c) film showed a contact angle of 36.2°, indicating better hydrophilicity or biocompatibility than SWCNHs. Meanwhile, the hybrid had a better dispersion than single SWCNHs in water (Fig. 3B), and was stable for at least two weeks due to the electrostatic repulsion. The improved biocompatibility and dispersion of the hybrid could greatly enhance the loading capacity of protein and preserve the bioactivity of the immobilized biomolecules, thus providing a desirable platform for biosensing application.

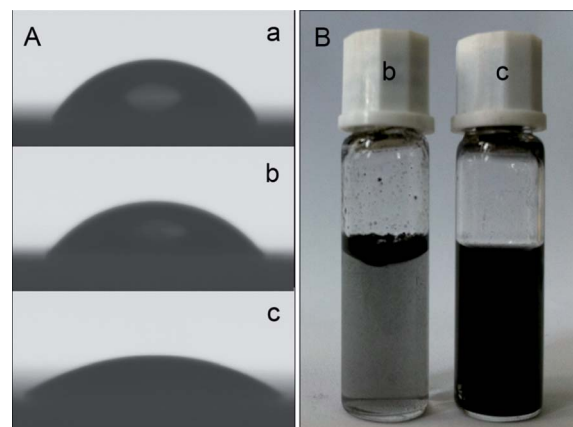


Fig. 3 (A) Contact angle photographs of bare (a), SWCNH (b), GNP-SWCNH (c) modified substrates, and (B) photographs of water dispersions (1 mg mL⁻¹) of SWCNHs (b) and GNPs-SWCNH (c).

Electrocatalytic oxidation of H₂O₂ and UA

The sensitive and reliable determination of H₂O₂ and UA is of importance for further application in bioanalysis, particularly for detection of hypoxanthine and xanthine which can be oxidized by dissolved oxygen to produce H₂O₂ and UA in the presence of XOx. The bare Pt electrode exhibited a good anodic response to H₂O₂ at +0.43 V (Fig. 4A, curve a). When SWCNHs were modified on the electrode, the peak current slightly decreased due to a blocking effect of SWCNH on the catalytic oxidation of H₂O₂ (Fig. 4A, curve b). In contrast, the GNPs-SWCNH modified electrode showed an enhanced peak current and the anodic potential shifted negatively to +0.34 V (Fig. 4A, curve c), which should be attributed to the fact that the GNPs at the Pt electrode have an electrocatalytic effect on the oxidation of H₂O₂ (Fig. 4A, curve d).¹⁹ This value was much lower than +0.57 V at the gold-deposited polyvinylferrocene modified platinum electrode, and +0.61 V at the cation-exchange polymeric film modified platinum electrode.²⁰ This means that the GNP-SWCNH modified electrode has high electrocatalytic activity toward oxidation of H₂O₂, which is beneficial for further preparation of the biosensor.

UA could be oxidized at +0.48 V at the bare Pt electrode (Fig. 4B, curve a). After the electrode was coated with SWCNHs, the oxidation current of UA increased, and the anodic peak

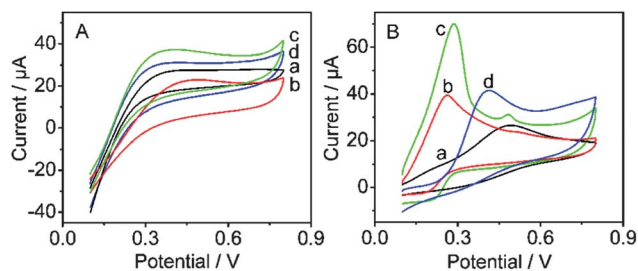


Fig. 4 The electrocatalytic oxidation of bare (a), SWCNH modified (b), GNP-SWCNH modified (c) and GNP modified (d) platinum electrodes in (A) 3.0 mM H₂O₂ and (B) 3.0 mM uric acid in 0.05 M PBS. Scan rate: 100 mV s⁻¹.

potential shifted negatively to +0.26 V (Fig. 4B, curve b), indicating the electrocatalytic activity of SWCNHs toward the oxidation of UA. The GNP-SWCNH modified platinum electrode exhibited a dramatically increasing current with a slightly positive shift of the anodic potential to +0.28 V (Fig. 4B, curve c), which is lower than +0.37 V at the poly(*N*-methylpyrrole)-Pd-nanoclusters modified platinum electrode, and +0.56 V at the fluorosurfactant modified platinum electrode.²¹ Moreover, the electrocatalytic peak current for UA at the hybrid modified electrode was twice higher than that at the bare electrode, and the electrocatalytic peak potential at the hybrid modified electrode negatively shifted by 0.14 V in comparison to that at the GNPs modified electrode (Fig. 4B curve d). These results illustrated that the hybrid modified electrode possessed good electrocatalytic activity toward oxidation of both H₂O₂ and UA.

EIS characterization of the biosensor

In the classical Fe(CN)₆^{3-/4-} system, the Nyquist plots of different electrodes in the frequency range from 10⁻² to 10⁵ are shown in Fig. 5. The electron transfer resistance, *R*_{ct}, could be calculated from the equivalent circuit (inset in Fig. 5). At the bare Pt electrode, the redox process of the probe showed an electron transfer resistance of about 125 Ω (Fig. 5, curve a). After the GNP-SWCNH hybrid was coated on the electrode, it showed the minimum resistance value (Fig. 5, curve b), suggesting that the GNP-SWCNH hybrid accelerated the electron transfer between the redox probe and electrode surface. After XOx was coated on GNP-SWCNH modified electrode, the electron transfer resistance became 760 Ω due to the poor conductivity of protein (Fig. 5, curve c). In order to improve the stability of the biosensor, a film of PDDA was further coated to prevent the leakage of XOx on the XOx-GNP-SWCNH modified electrode, which led to an electron transfer resistance of 1050 Ω (Fig. 5, curve d). The increasing resistance value indicated the successful assembly of the biosensor. Moreover, this frame of

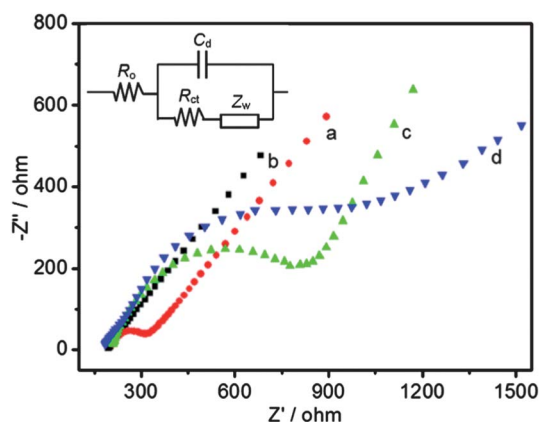


Fig. 5 EIS of bare (a), GNP-SWCNH modified (b), XOx-GNP-SWCNH modified (c), and PDDA-XOx-GNP-SWCNH modified (d) platinum electrodes in 0.1 M KNO₃ containing 5 mM K₃[Fe(CN)₆]/K₄[Fe(CN)₆]. Inset: equivalent circuit applied to fit impedance measurements. *R*_s, the resistance of the electrolyte solution; *C*_d, double-layer capacitance; *Z*_w, Warburg impedance; *R*_{ct}, electron transfer resistance.

PDDA-XOx-GNP-SWCNHs provided a microenvironment to maintain the bioactivity of XOx for rapid amperometric response towards the substrate.

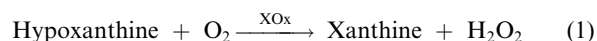
Condition optimization for amperometric detection

In order to obtain the efficient response of the PDDA-XOx-GNP-SWCNH modified electrode to the oxidation of hypoxanthine, the effect of pH on the response was investigated in the range of 5.0 to 9.0 using three modified electrodes (Fig. 6A). The current increased as the pH changed from 5.0 to 7.4, followed by a fast decrease in the pH range of 7.4–9.0. The maximum enzymatic response was obtained at pH 7.4. Therefore, pH 7.4 PBS was used for the next optimization experiment.

The dependence of the biosensor on potential was measured over the range of +0.2 V to +0.6 V as shown in Fig. 6B. The amperometric response of the biosensor to hypoxanthine increased with the increasing potential from +0.2 to +0.4 V and tended to a plateau after +0.4 V. Thus, the optimum applied potential was +0.4 V, which is lower than +0.55 V at the copolymer functionalized graphene modified platinum electrode.^{3a} This low applied potential is beneficial for the elimination of the interference in detection of real samples.

Analytical performance of the biosensor

In the presence of XOx hypoxanthine can be oxidized in air-saturated PBS to generate H₂O₂ and UA according to the following equations:



Therefore, both hypoxanthine and xanthine can be detected by measuring the oxidation current of H₂O₂ and UA at the XOx-GNP-SWCNH modified electrode.

The typical amperometric response of the biosensor to hypoxanthine was determined by the successive additions of hypoxanthine into 8 mL of 50 mM pH 7.4 PBS under the optimum conditions. As shown in Fig. 7A, the response of the biosensor at +0.4 V increased and reached a steady state. The linear range was from 1.5 to 35.4 μM with a detection limit of 0.61 μM (*S/N* = 3). The sensitivity of the sensor for hypoxanthine was 202.4 mA M⁻¹ cm⁻², which was higher than 101.9 mA M⁻¹ cm⁻²

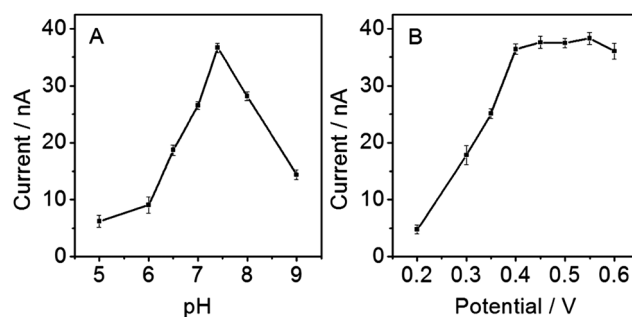


Fig. 6 Optimization of (A) pH and (B) detection potential of the biosensor in air-saturated 0.05 M PBS buffer containing 5.0 μM hypoxanthine (*n* = 3).

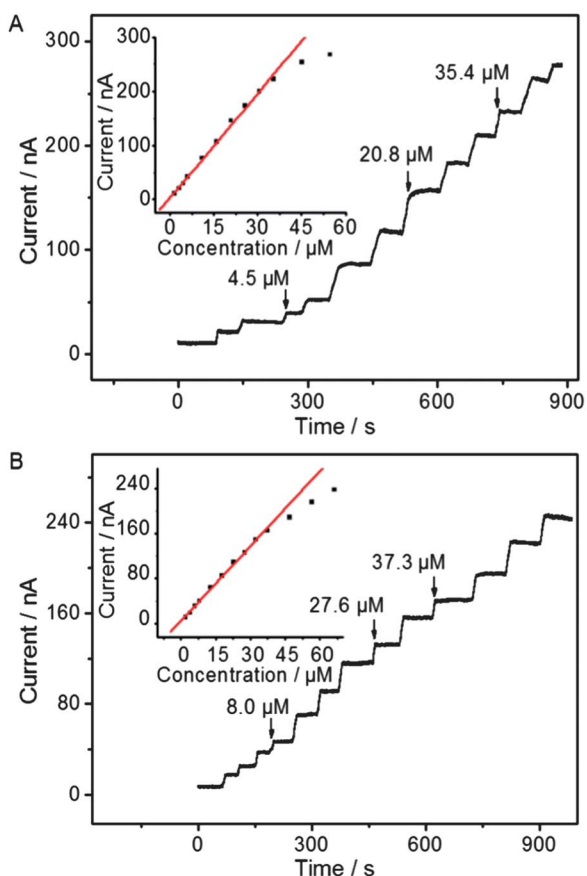


Fig. 7 Typical current–time response curves of the biosensor upon successive additions of (A) hypoxanthine and (B) xanthine. Insets: linear calibration curves. Applied potential: +0.40 V.

at the Nafion–XOx–Au colloid chemically modified biosensor.¹⁹ At the same optimized conditions, the linear range and detection limit for xanthine detection were 2.0 to 37.3 μM and 0.72 μM, respectively (Fig. 7B). The sensitivity of the sensor for xanthine was 141.1 mA M^{−1} cm^{−2}, which was also higher than 8.2 mA M^{−1} cm^{−2} at the supramolecular-based biosensor,²² and 29.0 and 53.1 mA M^{−1} cm^{−2} at the gold and platinum nanoparticles/polyvinylferrocene modified electrode, respectively.²³

The repeatability of the biosensor was examined at the hypoxanthine concentrations of 5 and 10 μM, and the relative standard deviations for five determinations were 2.4% and 1.8%, respectively. In addition, the relative standard deviation of current signals for the measurement of 5 μM hypoxanthine at five independently prepared biosensors was 5.3%, which indicated good reproducibility of the biosensor preparation. When the biosensor was stored in 0.05 M pH 7.0 PBS at 4 °C, and used once every 7 days, the enzyme electrode retained 95% and 88% of its initial activity after one and two weeks, respectively. These results indicated acceptable stability.

Real sample analysis

To evaluate the analytical reliability and application potential of the proposed method, the biosensor was employed to detect hypoxanthine in the fish sample. The concentration of hypoxanthine in the fresh fish sample was around 5.0 μM.^{3a,16}

However, due to the lack of enough sensitivity, recovery testing was carried out by testing the mixture of the fish sample and standard hypoxanthine solution in 0.1 M pH 7.4 PBS. At the concentration of 5 μM and 20 μM the recoveries were 96.4 ± 0.4% and 98.3 ± 0.6% (*n* = 3), respectively, which indicated acceptable precision and the possibility for real analytical application.

Conclusions

A novel GNPs–SWCNH hybrid was proposed for the fabrication of a biosensing platform. The homogeneous dispersion and nanoporous construction of the GNPs–SWCNH hybrid offered a good environment for enzyme immobilization. Based on the good biocompatibility, conductivity and large surface-to-volume ratio, the hybrid modified electrode possessed excellent electrocatalytic activity toward oxidation of both H₂O₂ and UA. By integrating with the enzymatic reaction of xanthine oxidase, a biosensor with good performance for the detection of hypoxanthine and xanthine was proposed. The biosensor showed low applied potential, high reproducibility, and acceptable recovery. The GNP functionalized SWCNHs provided a convenient and low-cost platform for biosensing application.

Acknowledgements

This work was funded by National Natural Science Foundation of China (21121091, 21135002, 21075060), and Natural Science Foundation of Jiangsu (BK2010302).

Notes and references

- (a) Z. Liu, X. M. Sun, N. Nakayama-Ratchford and H. J. Dai, *ACS Nano*, 2007, **1**, 50; (b) D. Eder, *Chem. Rev.*, 2010, **110**, 1348; (c) W. M. Zhang, P. Sherrell, A. I. Minett, J. M. Razal and J. Chen, *Energy Environ. Sci.*, 2010, **3**, 1286.
- (a) S. Tang, X. Z. Wang, J. P. Lei, Z. Hu, S. Y. Deng and H. X. Ju, *Biosens. Bioelectron.*, 2010, **26**, 432; (b) J. M. Shen and Y. T. Feng, *J. Phys. Chem. C*, 2008, **112**, 13114; (c) Z. P. Wang, M. Shoji and H. Ogata, *Analyst*, 2011, **136**, 4903.
- (a) J. Zhang, J. P. Lei, R. Pan, Y. D. Xue and H. X. Ju, *Biosens. Bioelectron.*, 2010, **26**, 371; (b) D. A. C. Brownson and C. E. Banks, *Analyst*, 2010, **135**, 2768; (c) R. S. Dey, S. Hajra, R. K. Sahu, C. R. Raj and M. K. Panigrahi, *Chem. Commun.*, 2012, **48**, 1787; (d) H. C. Chang, X. J. Wu, C. Y. Wu, Y. Chen, H. Jiang and X. M. Wang, *Analyst*, 2011, **136**, 2735; (e) K. Wang, H. N. Li, J. Wu, C. Ju, J. J. Yan, Q. Liu and B. J. Qiu, *Analyst*, 2011, **136**, 3349.
- S. Y. Zhu, W. X. Niu, H. J. Li, S. Han and G. B. Xu, *Talanta*, 2009, **79**, 1441.
- J. M. Jiménez-Soto, Y. Moliner-Martínez, S. Cárdenas and M. Valcárcel, *Electrophoresis*, 2010, **31**, 1681.
- P. Hiralal, H. L. Wang, H. E. Unalan, Y. L. Liu, M. Rouvala, D. Wei, P. Andrew and G. A. J. Amaratunga, *J. Mater. Chem.*, 2011, **21**, 17810.
- D. Wen, X. L. Xu and S. J. Dong, *Energy Environ. Sci.*, 2011, **4**, 1358.
- S. Y. Zhu, H. J. Li, W. X. Niu and G. B. Xu, *Biosens. Bioelectron.*, 2009, **25**, 940.
- (a) G. Mountrichas, T. Ichihashi, S. Pispas, M. Yudasaka, S. Iijima and N. Tagmatarchis, *J. Phys. Chem. C*, 2009, **113**, 5444; (b) G. Pagona, A. S. D. Sandanayaka, Y. Araki, J. Fan, N. Tagmatarchis, M. Yudasaka, S. Iijima and O. Ito, *J. Phys. Chem. B*, 2006, **110**, 20729.
- (a) J. Zhang, J. P. Lei, R. Pan, C. Leng, Z. Hu and H. X. Ju, *Chem. Commun.*, 2011, **47**, 668; (b) L. Ding, Q. J. Ji, R. C. Qian, W. Cheng and H. X. Ju, *Anal. Chem.*, 2010, **82**, 1292.
- N. Sano and S. Ukita, *Mater. Chem. Phys.*, 2006, **99**, 447.

- 12 C. Poonjarernsilp, N. Sano, T. Charinpanitkul, H. Mori, T. Kikuchi and H. Tamon, *Carbon*, 2011, **49**, 4920.
- 13 A. S. Hernández-Cázares, M. Aristoy and F. Toldrá, *Food Chem.*, 2010, **123**, 949.
- 14 (a) P. N. Bjerring, J. Hauerberg, L. Jørgensen, H. Frederiksen, F. Tofteng, B. A. Hansen and F. S. Larsen, *J. Hepatol.*, 2010, **53**, 1054; (b) D. Farthing, D. Sica, T. Gehr, B. Wilson, I. Fakhry, T. Larus, C. Fathing and H. T. Karnes, *J. Chromatogr., B: Anal. Technol. Biomed. Life Sci.*, 2007, **854**, 158; (c) N. Cooper, R. Khosravan, C. Erdmann, J. Fiene and J. W. Lee, *J. Chromatogr., B: Anal. Technol. Biomed. Life Sci.*, 2006, **837**, 1.
- 15 (a) B. C. Yoo, S. Y. Kong, S. G. Jang, K. H. Kim, S. A. Ahn, W. S. Park, S. Park, T. Yun and H. S. Eom, *BMC Cancer*, 2010, **10**, 55; (b) M. Clariana, M. Gratacós-Cubarsí, M. Hortós, J. A. García-Regueiro and M. Castellari, *J. Chromatogr., A*, 2010, **1217**, 4294; (c) L. C. Sander, M. Bedner, M. C. Tims, J. H. Yen, D. L. Duewer, B. Porter, S. J. Christopher, R. D. Day, S. E. Long, J. L. Molloy, K. E. Murphy, B. E. Lang, R. Lieberman, L. J. Wood, M. J. Payne, M. C. Roman, J. M. Betz, A. NguyenPho, K. E. Sharpless and S. A. Wise, *Anal. Bioanal. Chem.*, 2012, **402**, 473; (d) M. Kathiwala, A. O. Affum and A. Brajter-Toth, *Anal. Bioanal. Chem.*, 2010, **396**, 1763.
- 16 Y. Y. Zhang, S. Y. Deng, J. P. Lei, Q. N. Xu and H. X. Ju, *Talanta*, 2011, **85**, 2154.
- 17 (a) W. Cheng, Y. L. Chen, F. Yan, L. Ding, S. J. Ding, H. X. Ju and Y. B. Yin, *Chem. Commun.*, 2011, **47**, 2877; (b) S. M. Bonk and F. Lisdat, *Biosens. Bioelectron.*, 2009, **25**, 739.
- 18 (a) H. C. Choi, M. Shim, S. Bangsaruntip and H. J. Dai, *J. Am. Chem. Soc.*, 2002, **124**, 9058; (b) X. H. Peng, J. Y. Chen, J. A. Misewich and S. S. Wong, *Chem. Soc. Rev.*, 2009, **38**, 1076; (c) X. Yang, M. S. Xu, W. M. Qiu, X. Q. Chen, M. Deng, J. L. Zhang, H. Iwai, E. Watanabe and H. Z. Chen, *J. Mater. Chem.*, 2011, **21**, 8096; (d) Z. G. Gu, S. P. Yang, Z. J. Li, X. L. Sun, G. L. Wang, Y. J. Fang and J. K. Liu, *Electrochim. Acta*, 2011, **56**, 9162.
- 19 G. Y. Shi, M. Liu, M. Zhu, T. S. Zhou, J. S. Chen, L. T. Jin and J. Y. Jin, *Analyst*, 2002, **127**, 396.
- 20 (a) M. T. Sulak, Ö. Gökdogan, A. Gülce and H. Gülce, *Biosens. Bioelectron.*, 2006, **21**, 1719; (b) M. F. S. Teixeira, F. H. Cincotto and P. A. Raymundo-Pereira, *Electrochim. Acta*, 2011, **56**, 6804.
- 21 (a) N. F. Atta, M. F. El-Kady and A. Galal, *Anal. Biochem.*, 2010, **400**, 78; (b) Z. F. Chen and Y. B. Zu, *J. Electroanal. Chem.*, 2007, **603**, 281.
- 22 R. Villalonga, M. Matos and R. Cao, *Electrochem. Commun.*, 2007, **9**, 454.
- 23 S. Z. Baş, H. Glüce, S. Yıldız and A. Gülce, *Talanta*, 2011, **87**, 189.